Supporting Information

Scholz *et al.* 10.1073/pnas.0807841105

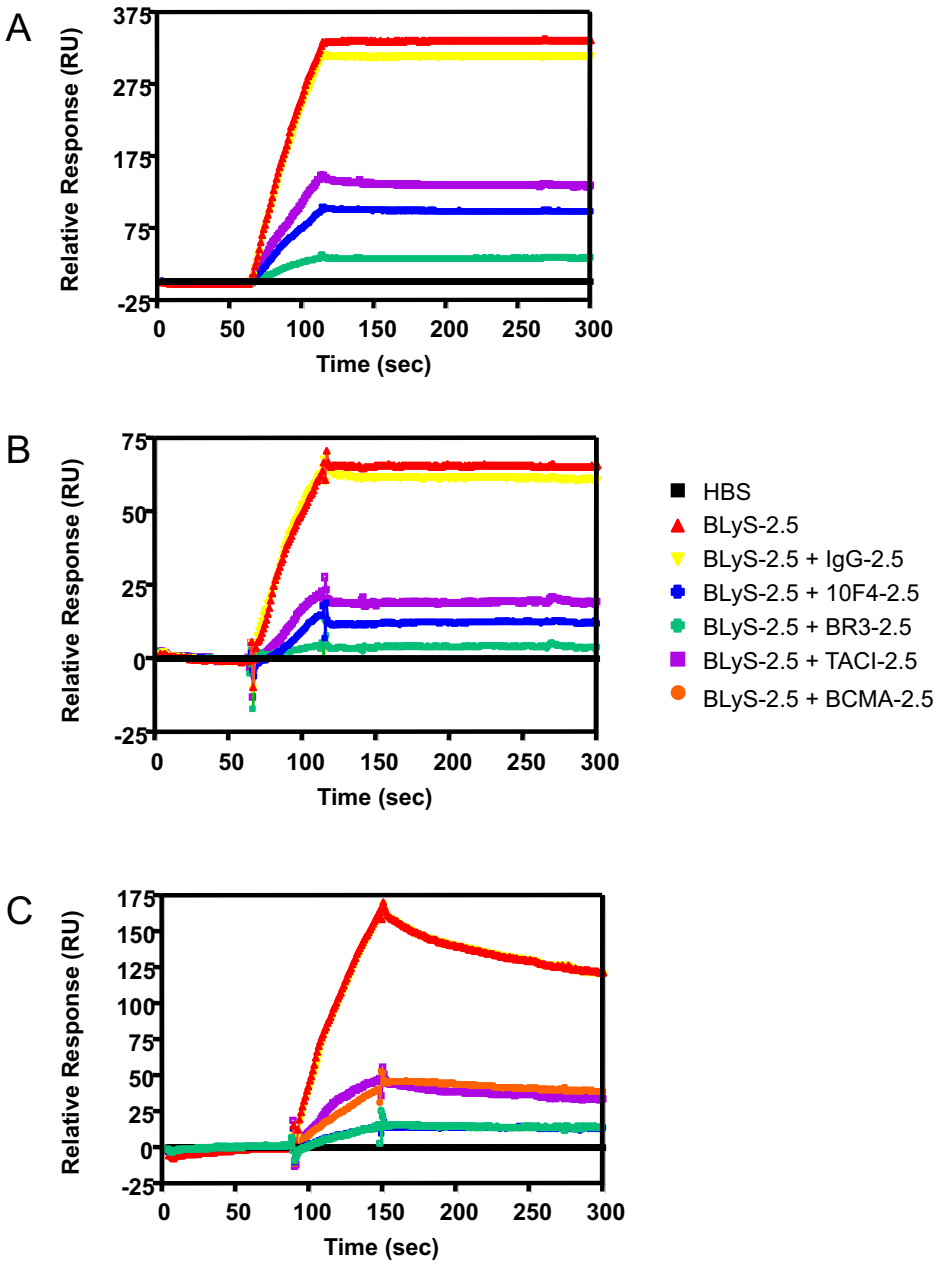

Fig. S1. Inhibition of murine BLyS binding to murine BR3 (*A*), murine TACI (*B*), and murine BCMA (*C*). Direct binding of BLyS over an immobilized BLyS receptor surface was assessed in the presence of murine BLyS receptor Fc, 10F4, or an isotype antibody control. Competitive binding was measured by relative ranking of bound BLyS in the presence of inhibitor compared to the isotype control. Soluble BLyS receptor Fc was covalently immobilized over a CM5 chip to a target density of ≈2,000 relative units (RU). A total of 2.5 μg/ml BLyS was preincubated with and without the same concentration of competitor (1:1, vol/vol) outside the instrument. After 15 min of incubation at ambient temperature, samples were injected over the immobilized flow cell at 30 μl/min for 0.85 min. The surface was washed for 2.5 min with Hepes-buffered saline (HBS) to measure the off-rate of bound antigen (BLyS).

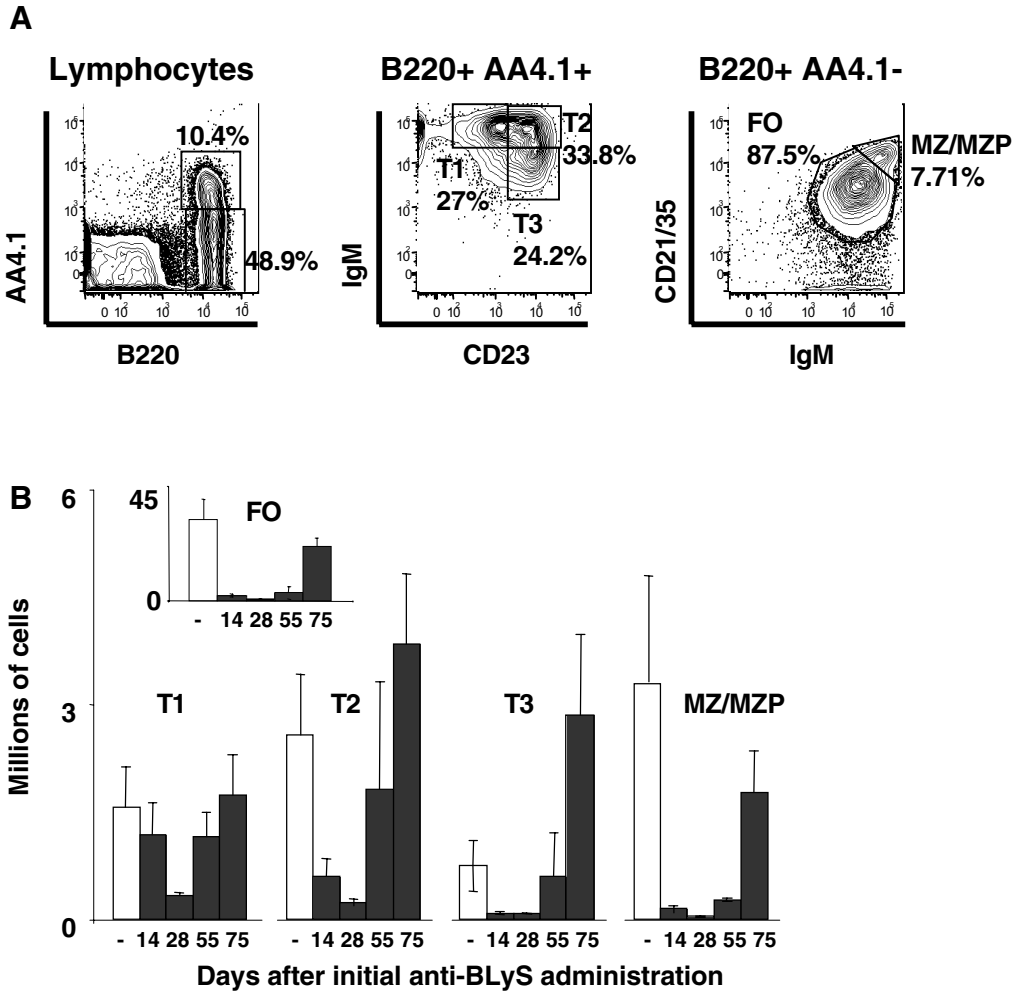

Fig. S2. Effects of BLyS neutralization on B cell subsets. C57BL/6 mice were treated with 100 μg of anti-BLyS i.p. on days 0 and 5 and subsequently analyzed. (*A*) Splenocytes were analyzed by flow cytometry using the gating scheme shown. Single, live lymphocytes were gated by FSC and SSC profile and DAPI exclusion. Axes are on a 5-log scale. T1, T2, and T3 are transitional B cell subsets, and FO (follicular) and MZ/MZP (marginal zone/marginal zone precursors) are mature subsets. Phenotyping strategies used the following antibodies: FITC-anti (α)-CD43 and α-CD4, PE-α-CD8, biotinylated α-CD23 and α-CD3 (BD Biosciences), PE-Cy7-α-IgM, and PE-Texas Red-Streptavidin (BD Pharmingen); PE-α-mouse lambda (Southern Biotechnology Associates); and APC-α-AA4.1 and APC-Cy5.5-α-B220 (eBioscience). PE-Cy5.5-α-CD21/35 was a gift of D. Allman (University of Pennsylvania, Philadelphia). (*B*) Total splenic numbers for each B cell subset identified in *A* are shown. Bars show numbers $\pm$ SD for six untreated mice (open bars) and three treated mice (filled bars).

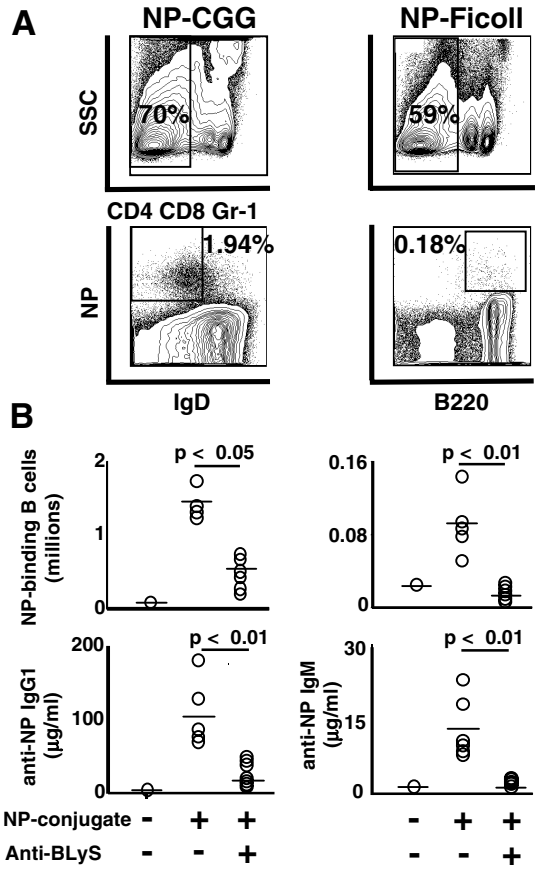

Fig. S3. Primary humoral immune responses are attenuated in anti-BLyS-treated mice. C57BL/6 mice were immunized with either NP-CGG in alum (TD antigen) or NP-Ficoll in saline (TI antigen) 28–30 days after anti-BLyS treatment. (*A*) Seven days after immunization, splenic NP-binding B cells were identified by the gating scheme shown. Single, live lymphocytes were gated by FSC and SSC profile and DAPI exclusion; NP-binding B cells were identified as $CD4^-$ $CD8^-$ $GR1^-$ IgD^- NP^+. These cells were also λ^+ $Ig\beta^+$ (data not shown). (*B*) Numbers of NP-binding splenic B cells (*Upper*) and levels of serum NP-specific antibody (*Lower*) after challenge with NP conjugate in mice treated as shown at the bottom. Each point represents one mouse, with the average for a treatment group indicated by a horizontal bar. Plates were coated with 10 μg/ml NP_3BSA (to detect high-affinity IgG_1 in TD responses) or NP_{30} (to detect IgM in TI responses) in 100 mM bicarbonate buffer and blocked with 2% BSA in PBS, and serum dilutions were incubated for 1 h. NP-specific IgM and IgG_1 standards were a gift of G. Kelsoe (Duke University). HRP-conjugated goat anti-mouse IgM or IgG_1 (Southern Biotechnology Associates) was used for detection with a TMB substrate kit (BD Biosciences). Washes were performed using PBS plus 0.1% Tween 20.

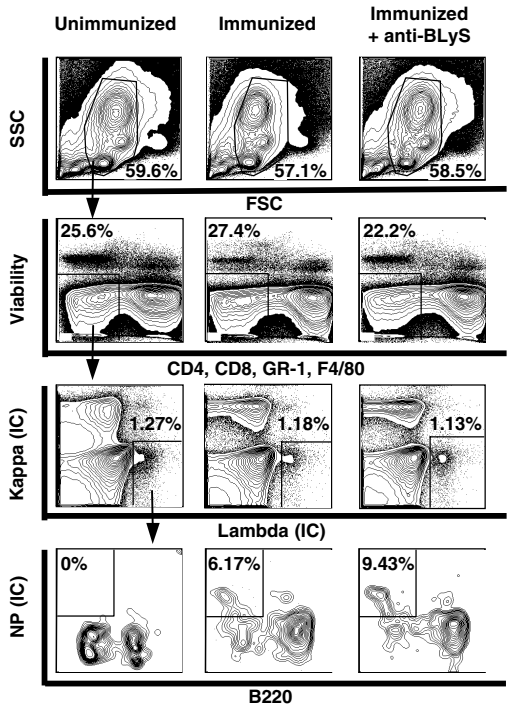

Fig. S4. Gating strategy and representative data for identification of NP-specific long-lived plasma cells in bone marrow. Single lymphocytes were gated by FSC and SSC profile. Live $CD4^-$ $CD8^-$ $GR\text{-}1^-$ $F4/80^-$ cells were further gated as intracellular $\kappa(IC)^+$, IC λ^+. NP-specific plasma cells were identified as $B220^-$ intracellular NP^+.

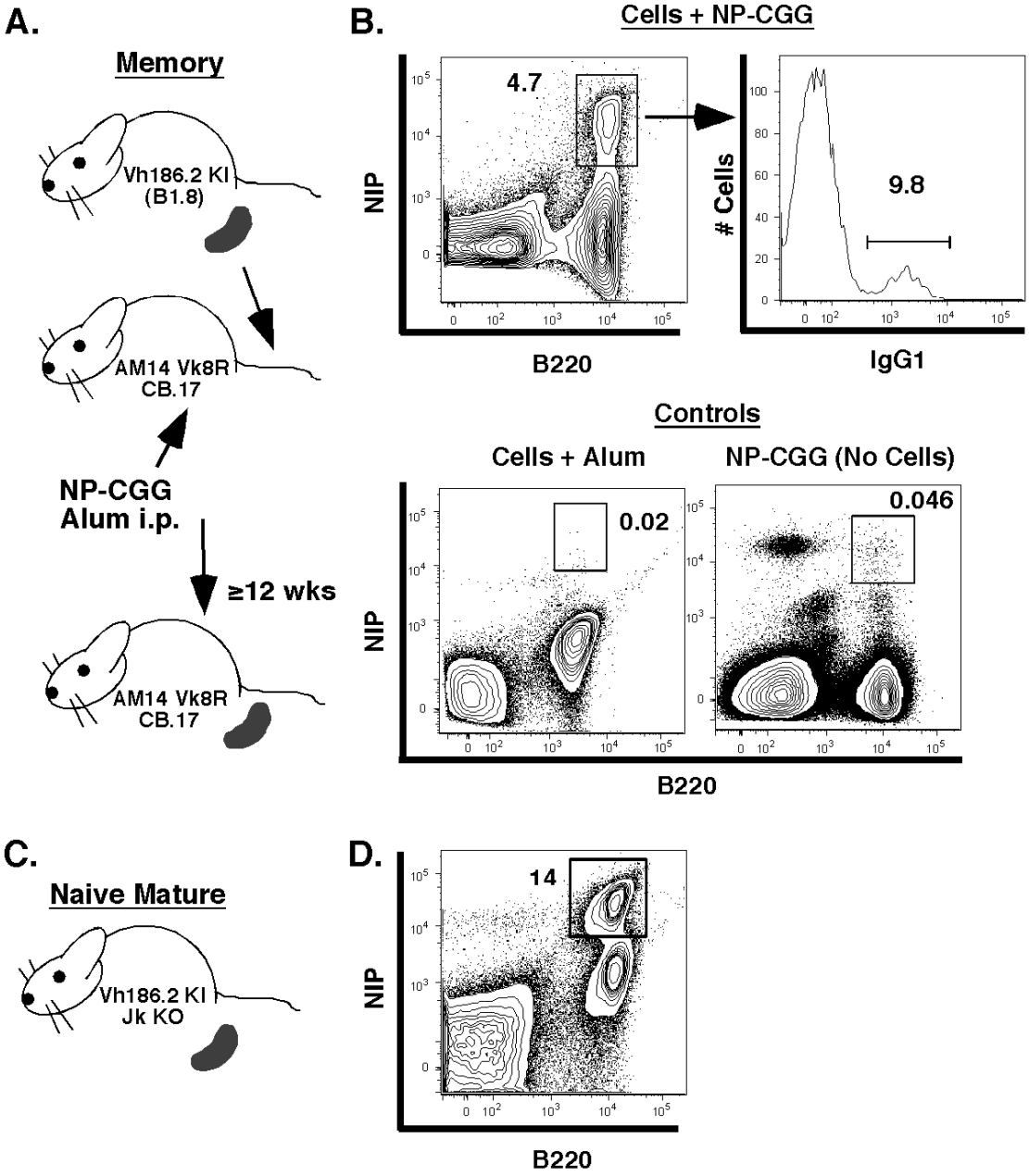

Fig. S5. Generation of memory B cells from NP-specific Vh186.2 KI-bearing precursors in an adoptive transfer system (Memory System 3). (*A*) Schematic of use of cell transfer system to generate NP-specific memory B cells in the absence of newly generated naïve NP-specific B cells. (*B*) FACS profiles of live-gated recipient splenocytes >12 weeks after cell transfer and immunization (*Upper*) versus cell transfer and sham immunization with alum alone (*Lower Left*) versus immunization without cell transfer (*Lower Right*). There is an expanded population of NIP-binding splenic B cells in transferred, immunized mice. Some of these cells are class-switched to IgG_1. In the absence of immunization, only a negligible population of donor NP-specific B cells persists. Recipient mice not transferred with Vh186.2 KI splenocytes mount a weak response to NP-CGG; the $B220^-$ NIP-binding population to the left of the gate represents cytophilic antibody binding to non-B cells. (*C*) Naïve NP-specific B cells were purified from spleens of unimmunized 7- to 10-week-old Vh186.2 KI $J\kappa$ KO mice. (*D*) FACS profiles of live-gated naïve NP-specific B splenic B cells from unimmunized donor-strain mice demonstrate an enriched population of NP-binding B cells.